INSTITUTE OF PHYSICS PUBLISHING JOURNAL OF OPTICS B: QUANTUM AND SEMICLASSICAL OPTICS

J. Opt. B: Quantum Semiclass. Opt. **7** (2005) 43–53 doi:10.1088/1464-4266/7/2/003

Non-Markovian theory of relativistic electric-dipole spontaneous emission of hydrogen-like atoms

Chang-qi Cao[1], Xiao-wei Fu[2] and Hui Cao[3]

[1] Department of Physics, Peking University, Beijing 100871, People's Republic of China
[2] Department of Physics, Tsinghua University, Beijing 100084, People's Republic of China
[3] Department of Physics and Astronomy, Northwestern University, Evanston, IL 60208-3112, USA

E-mail: cqcao@pku.edu.cn and h-cao@northwestern.edu

Received 30 June 2004, accepted for publication 8 December 2004
Published 6 January 2005
Online at stacks.iop.org/JOptB/7/43

Abstract
The non-Markovian corrections to electric-dipole emission of hydrogen-like atoms of large atomic number Z are studied by multipole photon field formulation. The correlation functions are derived by the corresponding spectra, which show how the δ-function type correlation is approached. The decay of upper-level population is calculated by the relevant integro-differential equation. The numerical results show that the relativistic and finite atom-size corrections are evident; while the non-Markovian corrections are negligible in the main period of decay, they can manifest themselves in the far remote tail.

Keywords: spontaneous emission, relativistic, non-Markovian

1. Introduction

The famous Weisskopf–Wigner theory of atomic spontaneous emission [1] is founded by the following two presuppositions: first, assuming the decay rate of the upper-level population N_2 is proportional to the instantaneous value of N_2, with no reference to its past history; second, in evaluating the decay rate, the atom is taken as a point-like electric-dipole, neglecting its finite dimension as compared with the wavelength of the emitted light. The first one is actually the Markovian approximate result of the integro-differential equation which relates the time derivative of N_2 to its past values. The second presupposition leads directly to the result that the decay rate is just the Einstein A coefficient γ_A. Apart from these two points, the effect of electron spin is not taken into account.

As is well known, a dynamic system with spectrum bounded below could not have a purely exponential decay [2]. To find out the deviation from Weisskopf–Wigner law, quite a few authors restudied this problem in the 1970s–1990s [3–8]. All of these investigations applied the method of Laplace transformation to solve the relevant integro-differential equations, and various kinds of approximation were made in the inverse transformation. The deviations from the Weisskoff–Wigner law they obtained are mostly very small, except at the very beginning of the decay within a small interval of order $1/\omega_0$, and, as some of them claimed, also in the far remote tail of the decay in which N_2 is extremely small.

Most of these authors take the atomic number Z equal to unity in their investigation. We know the radius a of the electron cloud is proportional to Z^{-1}, and the emission frequency ω_0, which is proportional to the atomic level-energy difference, is in direct proportion to Z^2, leading to linear increase of $\omega_0 a/c$ with Z. This means the point-like electric-dipole approximation may possibly become poor for large Z. As to the Markov approximation, the actual correlation interval is assumed to be of order $1/\omega_0$, while the atomic decay time is of order $1/\gamma_A$. Therefore the validity of the Markov approximation requires their ratio $\gamma_A/\omega_0 \ll 1$. In the case of the hydrogen-like atom, γ_A is proportional to $\omega_0^3 a^2$, so that γ_A/ω_0 varies as Z^2. Hence any meaningful non-Markovian effect can only show itself for large Z.

Recently two of us (Cao and Cao) and other co-workers restudied this topic by totally different approaches [9, 10]. In [9], the generalized quantum stochastic trajectory analysis [11, 12] is employed. The obtained correction due

to the finite size of atom is calculated analytically and hence is reliable, to the extent that the Schrödinger equation is applicable. The corrections due to the non-Markovian effect so obtained however suffer from two problems as described in [10]. The first one lies in that the random number in the interval (0, 1) used in stochastic trajectory analysis is actually program generated; it will lead to errors when the times of utilization become large. The second problem comes from the simulation of the real non-Markovian correlation spectrum by a sum of several Lorentzian spectra. These two factors, especially the first one, make the calculated non-Markovian correction not so reliable. However, this method has the merit that it may take the effect of anti-rotating interactions into account [12] and hence has its own prospect. In [10] two of us and a co-worker first show the correlation function explicitly and then solve the relevant integro-differential equation by direct numerical calculation. In this way, one may get not only a concrete picture of the correlation function but also more accurate numerical results. However, the atomic states are still described by non-relativistic Schrödinger wavefunctions without spin degree of freedom, while for large Z the relativistic correction may be important.

In this paper, we will carry out the non-Markovian investigation of relativistic electric-dipole spontaneous emission, in which the photon field with total angular momentum $J = 1$ and parity $P = -1$ is used.

We note that to our knowledge this is the first time the non-Markovian effect in relativistic formulation has been investigated. Although [8] claims its correlation function is relativistic, actually it just includes the spin interaction term, still being non-relativistic.

2. General formulations

In general the multipole photon field describes a photon with definite wavelength, total angular momentum and parity. The corresponding vector potential will be denoted by $\mathbf{A}_{kJMP}(\mathbf{x})$, the combined index ($J = 1, M = \pm 1, 0, P = -1$) refers to electric-dipole field, ($J = 1, M = \pm 1, 0, P = +1$) refers to magnetic-dipole field and ($J = 2, M = \pm 2, \pm 1, 0, P = +1$) refers to the electric-quadrupole field. If we normalize the photon field in a large sphere of radius R_0 (with the atom at the centre), k will take discrete values. The concrete orthonormalization condition is as follows: write

$$\mathbf{A}_{kJMP}(\mathbf{x}) = \sqrt{\frac{2\pi\hbar c}{k}}\mathbf{F}_{kJMP}(\mathbf{x}), \tag{1}$$

then $\mathbf{F}_{kJMP}(\mathbf{x})'s$ satisfy

$$\int \mathbf{F}^*_{kJMP}(\mathbf{x}) \cdot \mathbf{F}_{k'J'M'P'}(\mathbf{x})\, \mathrm{d}^3x = \delta_{kk'}\delta_{JJ'}\delta_{MM'}\delta_{PP'}; \tag{2}$$

the above volume integration is within the normalization sphere.

The $\mathbf{F}_{kJMP}$ are expressed by the spherical Bessel function $g_L(kr)$ and vector spherical function $\mathbf{Y}_{JLM}(\theta, \varphi)$ as

$$\mathbf{F}_{kJMP}(\mathbf{x}) = \begin{cases} \sqrt{\dfrac{2k^2}{R_0}}\, g_J(kr)\mathbf{Y}_{JJM}(\theta,\varphi), \\ \quad \text{for } P = (-1)^{J+1}; \\ \sqrt{\dfrac{2k^2}{R_0}}\Big[-\sqrt{\dfrac{J}{2J+1}}\, g_{J+1}(kr)\mathbf{Y}_{JJ+1m}(\theta,\varphi) \\ \quad + \sqrt{\dfrac{J+1}{2J+1}}\, g_{J-1}(kr)\mathbf{Y}_{JJ-1M}(\theta,\varphi)\Big], \\ \quad \text{for } P = (-1)^{J}, \end{cases} \tag{3}$$

where the vector spherical function $\mathbf{Y}_{JLM}(\theta, \varphi)$ is defined by

$$\mathbf{Y}_{JLM}(\theta,\varphi) = \sum_{\mu=0,\pm1} C^{JM}_{L(M-\mu),1\mu} Y_{L(M-\mu)}(\theta,\varphi)\mathbf{n}^{(\mu)}, \tag{4}$$

in which the $\mathbf{n}^{(\mu)}$ are spherical bases, and may be expressed by the usual rectangular bases $(\mathbf{n}_1, \mathbf{n}_2, \mathbf{n}_3)$ as

$$\mathbf{n}^{(+1)} = -\frac{1}{\sqrt{2}}(\mathbf{n}_1 + \mathrm{i}\mathbf{n}_2), \tag{5a}$$

$$\mathbf{n}^{(0)} = \mathbf{n}_3, \tag{5b}$$

$$\mathbf{n}^{(-1)} = \frac{1}{\sqrt{2}}(\mathbf{n}_1 - \mathrm{i}\mathbf{n}_2). \tag{5c}$$

After field quantization, the operator $\hat{\mathbf{A}}(\mathbf{x})$ is expanded by

$$\hat{\mathbf{A}}(\mathbf{x}) = \sum_{kJMP} [\hat{a}_{kJMP}\mathbf{A}_{kJMP}(\mathbf{x}) + \hat{a}^\dagger_{kJMP}\mathbf{A}^*_{kJMP}(\mathbf{x})]; \tag{6}$$

the $\hat{a}_{kJMP}$ and $\hat{a}^\dagger_{kJMP}$ are corresponding absorption and emission operators of photon.

As to the hydrogen-like atom, if only the two levels concerned need to be taken into account, the interaction Hamiltonian in the rotating-wave approximation may be written as

$$\hat{H}_{\mathrm{int}} = \mathrm{i}\hbar \sum_{kJMP} [g_{kJMP}\hat{\sigma}_+\hat{a}_{kJMP}\mathrm{e}^{-\mathrm{i}(\omega-\omega_0^{(\mathrm{R})})t} - g^*_{kJMP}\hat{\sigma}_-\hat{a}^\dagger_{kJMP}\mathrm{e}^{\mathrm{i}(\omega-\omega_0^{(\mathrm{R})})t}], \tag{7}$$

where $\hat{\sigma}_+$ and $\hat{\sigma}_-$ are atom level upward and downward change operators, $\omega_0^{(\mathrm{R})}$ is the relativistic value of $\frac{1}{\hbar}(E_2 - E_1)$, $\omega = kc$, and g_{kJMP} is the corresponding coupling constant, given by

$$g_{kJMP} = \frac{e}{\hbar}\int \mathrm{d}^3x\, \overline{\psi}_2(\mathbf{x})\gamma\psi_1(\mathbf{x}) \cdot \mathbf{A}_{kJMP}(\mathbf{x}), \tag{8}$$

in which $\psi_2(\mathbf{x})$ and $\psi_1(\mathbf{x})$ are the upper level and lower level atomic wavefunctions respectively; they are now four-component Dirac spinors. In equation (7), the anti-rotating interaction is omitted, since according to [13] its effect is negligibly small.

We express the state of our system as

$$|t\rangle = C_2(t)|\psi_2; 0\rangle + \sum_{kJMP} C_{1,kJMP}(t)|\psi_1; kJMP\rangle \tag{9}$$

where $|\psi_2; 0\rangle$ denotes the state in which the atom is in its upper level and no photon exists; $|\psi_1; kJMP\rangle$ denotes the state in

which the atom is in its lower level with one photon in the mode $(kJMP)$. The initial condition is

$$C_2(0) = 1, \qquad C_{1,kJMP}(0) = 0.$$

The coupled equations for $C_2(t)$ and $C_{1,kJMP}(t)$ can be readily deduced from $\hat{H}_{\rm int}$. We take the interaction picture in our formulation, hence

$$\begin{aligned} \frac{\mathrm{d}}{\mathrm{d}t}C_{1,kJMP}(t) &= -g^*_{kJMP}\mathrm{e}^{\mathrm{i}(\omega-\omega_0^{(\mathrm{R})})t}C_2(t), \\ \frac{\mathrm{d}}{\mathrm{d}t}C_2(t) &= \sum_{kJMP} g_{kJMP}\mathrm{e}^{-\mathrm{i}(\omega-\omega_0^{(\mathrm{R})})t}C_{1,kJMP}(t). \end{aligned} \tag{10}$$

After eliminating the variable $C_{1,kJMP}(t)$, the resultant integro-differential equation for $C_2(t)$ is given by

$$\frac{\mathrm{d}}{\mathrm{d}t}C_2(t) = -\int_0^t U(t-t')C_2(t')\,\mathrm{d}t'. \tag{11}$$

The function $U(t-t')$ is the so-called correlation function which correlates $\frac{\mathrm{d}}{\mathrm{d}t}C_2(t)$ with the past values of C_2, and is given by

$$U(t-t') = \sum_{kJMP} |g_{kJMP}|^2\mathrm{e}^{-\mathrm{i}(\omega-\omega_0^{(\mathrm{R})})(t-t')}. \tag{12}$$

The summation over (J, M, P) is actually limited in the values allowed by conservation laws.

When the radius R_0 of the normalized sphere is allowed to tend to infinity, the summation over k will be transferred to integration over ω according to the rule

$$\sum_k \to \frac{R_0}{\pi}\int_0^\infty \mathrm{d}k = \frac{R_0}{c\pi}\int_0^\infty \mathrm{d}\omega.$$

Hence the correlation function $U(t-t')$ turns out to be

$$U(t-t') = \int_0^\infty R(\omega)\mathrm{e}^{-\mathrm{i}(\omega-\omega_0^{(\mathrm{R})})(t-t')}\,\mathrm{d}\omega, \tag{13}$$

with

$$R(\omega) = \sum_{JMP}\frac{R_0}{c\pi}|g_{kJMP}|^2, \qquad \omega = kc. \tag{14}$$

$R(\omega)$ is called the spectrum of the correlation function, or for short the correlation spectrum. One main task of our paper is to deduce this correlation function by relativistic Dirac wavefunctions of the hydrogen-like atom.

In the case where the practical correlation time-interval, which will be denoted by $\tau_{\rm c}$, is much smaller than the decay time which is of order $1/\gamma_{\rm A}$, the inverse of the Einstein A coefficient, then $C_2(t')$ in equation (11) may be taken as $C_2(t)$ out of the integral, leading to

$$\frac{\mathrm{d}}{\mathrm{d}t}C_2(t) = -\beta_{\rm c}C_2(t), \tag{15a}$$

where

$$\beta_{\rm c} \cong \int_0^\infty U(\tau)\,\mathrm{d}\tau \equiv \beta \tag{15b}$$

for $t > \tau_{\rm c}$. Equation (15a) is the Markovian approximation of equation (11).

Substituting equation (13) into equation (15b) and change the order of integration, we obtain

$$\beta = \pi R(\omega_0^{(\mathrm{R})}) - \mathrm{i}\mathcal{P}\int_0^\infty \frac{R(\omega)}{\omega-\omega_0^{(\mathrm{R})}}\,\mathrm{d}\omega. \tag{15c}$$

Hence,

$$\begin{aligned} \frac{\mathrm{d}}{\mathrm{d}t}N_2(t) &= \left[\frac{\mathrm{d}}{\mathrm{d}t}C_2^*(t)\right]C_2(t) + C_2^*(t)\left[\frac{\mathrm{d}}{\mathrm{d}t}C_2(t)\right] \\ &\cong -(\beta^*+\beta)N_2(t) = -\gamma N_2(t) \end{aligned} \tag{16}$$

the constant $\gamma \equiv 2\,\mathrm{Re}\,\beta$ will be called the decay coefficient, and is given by

$$\gamma = 2\pi R(\omega_0^{(\mathrm{R})}), \tag{17}$$

according to equation (15c).

We may also relate γ to the correlation function as

$$\gamma = 2\int_0^\infty |U(\tau)|\cos\theta_U(\tau)\,\mathrm{d}\tau, \tag{18}$$

where $\theta_U(\tau)$ is the argument of $U(\tau)$, namely $U(\tau) = |U(\tau)|\mathrm{e}^{\mathrm{i}\theta_U(\tau)}$.

We see it is evident that for $t < \tau_{\rm c}$ the Markovian equation (15) is totally inapplicable, as it can be seen from equation (11) that $\frac{\mathrm{d}}{\mathrm{d}t}C_2(t)|_{t=0} = 0$, but this interval $(0, \tau_{\rm c})$ is actually too small to be recognized in the plotted decay curve. We will show in the ensuing paragraph that exponential decay is valid in the main part of the decay period even for $Z = 92$ (the largest real value). The remaining important thing to do is to calculate the relativistic value of γ with finite atom-volume effect taken into account.

3. The electric-dipole emission in atomic transition $2P_{3/2}$ to $1S_{1/2}$ and $2P_{1/2}$ to $1S_{1/2}$

For comparison with the non-relativistic results previously calculated [10], we still consider the electric-dipole emission in the transition of the hydrogen-like atom from 2P to 1S. Since the coupling of electron spin with the magnetic field intensity **B** in the photon field is not taken into account in hitherto non-relativistic calculations, including [10], the results given in all those papers are independent of the atomic total angular momentum j. Now in the present relativistic formulation, the electron current density $\overline{\psi}_2(\mathbf{x})\gamma\psi_1(\mathbf{x})$ does contain the spin current, so we should treat the transitions $2P_{3/2}$ to $1S_{1/2}$ and $2P_{1/2}$ to $1S_{1/2}$ separately.

First, let us argue that the corresponding two spontaneous emissions may be treated as a two-level process, thus the formulation of the last section may be applied. Under the rotating-wave approximation, the only other level that may be involved as an intermediate state is $2S_{1/2}$, whose relativistic energy is different from $2P_j$ ($j = 1/2, 3/2$). The atom may go back and forth between $2P_j$ and $2S_{1/2}$ for some time and finally transit from $2P_j$ to $1S_{1/2}$. However, the transition rate for $2P_j \to 2S_{1/2}$ is small, because the corresponding Einstein A coefficient is roughly equal to $(e^2/\hbar c)^3(1/4)[E(2P_j) - E(2S_{1/2})]/\hbar$ and the corresponding energy difference is small.

Now we consider the process $2P_{3/2}$ to $1S_{1/2}$. The Dirac wavefunction $1S_{1/2}$ is denoted by

$$\psi_1(\mathbf{x}) = \begin{pmatrix} \frac{1}{r}G_1(r)\Omega_{\frac{1}{2}0m}(\theta,\varphi) \\ \frac{1}{r}F_1(r)\Omega_{\frac{1}{2}1m}(\theta,\varphi) \end{pmatrix} \tag{19}$$

in which $\Omega_{jlm}(\theta,\varphi)$ represents the spherical spinor function with total angular momentum (j,m) and space parity $(-1)^l$, given by

$$\Omega_{jlm}(\theta,\varphi)=i^l\begin{pmatrix} C^{jm}_{l(m-\frac{1}{2}),\frac{1}{2}\frac{1}{2}}Y_{l(m-\frac{1}{2})}(\theta,\varphi)\\ C^{jm}_{l(m+\frac{1}{2}),\frac{1}{2}(-\frac{1}{2})}Y_{l(m+\frac{1}{2})}(\theta,\varphi)\end{pmatrix}. \tag{20}$$

The total parity of ψ_1 is (+1), since the lower Pauli spinor in ψ is of opposite intrinsic parity with respect to the upper Pauli spinor (as can be seen from the fact that intrinsic parity operator for Dirac wavefunction is γ_4).

The radial functions $G_1(r)$ and $F_1(r)$ can be found in many textbooks on quantum mechanics or relativistic quantum mechanics.

The Dirac wavefunction for $2P_{3/2}$ is similarly given by

$$\psi_2(\mathbf{x})=\begin{pmatrix}\frac{1}{r}G_2(r)\Omega_{\frac{3}{2}1m'}(\theta,\varphi)\\ \frac{1}{r}F_2(r)\Omega_{\frac{3}{2}2m'}(\theta,\varphi)\end{pmatrix}. \tag{21}$$

The emission frequency of this atomic transition is given by

$$\omega_0^{(\mathrm{R})}=\frac{1}{\hbar}(E_2-E_1)=\frac{m_0c^2}{\hbar}\left(\frac{1}{2}s_2-s_1\right) \tag{22}$$

where

$$s_1=\sqrt{1-Z^2\alpha^2},\qquad s_2=\sqrt{4-Z^2\alpha^2}. \tag{23}$$

Numerically we have

$$\omega_0^{(\mathrm{R})}=\begin{cases}0.201\dfrac{m_0c^2}{\hbar}, & \text{for } Z=92,\\ 0.052\dfrac{m_0c^2}{\hbar}, & \text{for } Z=50,\end{cases} \tag{24}$$

as compared with the non-relativistic values

$$\omega_0=\frac{3}{8}Z^2\alpha^2\frac{m_0c^2}{\hbar}=\begin{cases}0.169\dfrac{m_0c^2}{\hbar}, & \text{for } Z=92,\\ 0.050\dfrac{m_0c^2}{\hbar}, & \text{for } Z=50.\end{cases} \tag{25}$$

We see that the difference between $\omega_0^{(\mathrm{R})}$ and ω_0 is quite large, and according to equation (17) the value of $\omega_0^{(\mathrm{R})}$ is an important factor in determination of γ.

The photon emitted by this atomic transition may have two possible values of the combined index (J,P), namely $(1,-1)$ and $(2,-1)$, corresponding to electric-dipole and magnetic-quadrupole emission respectively.

Here we just consider the former; the latter must have an extremely small rate.

According to equation (14), the correlation spectrum for electric-dipole emission is given by

$$R(\omega)=\sum_M\frac{R_0}{c\pi}|g_{k1M(-1)}|^2,\qquad M=0,\pm1, \tag{26}$$

and from equations (8), (1), and (3)

$$g_{k1M(-1)}=2e\sqrt{\frac{\pi\omega}{3\hbar R_0}}\int\overline{\psi}_2(\mathbf{x})\gamma\psi_1(\mathbf{x})[\sqrt{2}g_0(kr)\mathbf{Y}_{10M}(\theta,\varphi)-g_2(kr)\mathbf{Y}_{12M}(\theta,\varphi)]\,\mathrm{d}^3x. \tag{27}$$

From the conservation of the third component of angular momentum, we have

$$M=m'-m. \tag{28}$$

The symmetry of space rotation implies that the final result should be independent of the third component of the total angular momentum of the whole system, which in our case is just m'. Hence we may choose $m'=\frac{3}{2}$ by will to make the allowed value of (M,m) just be $(1,\frac{1}{2})$. This means that among the three $g_{k1M(-1)}$ only $g_{k11(-1)}$ is non-zero, and hence

$$R(\omega)=\frac{R_0}{c\pi}|g_{k11(-1)}|^2. \tag{29}$$

The value of $g_{k11(-1)}$ can be evaluated directly according to the formula given above. After carrying out the integration over space coordinates we get

$$R(\omega)=|B_0B_0'|^2Z^2\alpha^3\frac{2\omega}{9\pi}\times\left|\frac{1}{1+s_1}S_0(\omega)+\frac{1}{4}\left(\frac{1}{1+s_1}-\frac{3}{2+s_2}\right)S_2(\omega)\right|^2, \tag{30}$$

in which

$$S_0(\omega)=\frac{1}{\mathrm{i}k}\left(\frac{2}{3}\right)^{s_1}\left(\frac{1}{3}\right)^{s_2}\Gamma(s_1+s_2)\times\left[\frac{1}{(1-\mathrm{i}ka)^{s_1+s_2}}-\mathrm{c.c.}\right], \tag{31a}$$

$$S_2(\omega)=-S_0(\omega)+\frac{3}{k^2a}\left(\frac{2}{3}\right)^{s_1}\left(\frac{1}{3}\right)^{s_2}\times\left[\frac{1}{\mathrm{i}ka}\frac{\Gamma(s_1+s_2-2)}{(1-\mathrm{i}ka)^{s_1+s_2-2}}-\frac{\Gamma(s_1+s_2-1)}{(1-\mathrm{i}ka)^{s_1+s_2-1}}+\mathrm{c.c.}\right] \tag{31b}$$

with

$$a=\frac{2a_B}{3Z}. \tag{32}$$

This parameter a is just equal to the non-relativistic transition radius of 2P to 1S.

Next, consider the process $2P_{1/2}$ to $1S_{1/2}$. The Dirac wavefunction for atomic initial state $2P_{1/2}$ is expressed by

$$\psi_2(\mathbf{x})=\begin{pmatrix}\frac{1}{r}G_2(r)\Omega_{\frac{1}{2}1m'}(\theta,\varphi)\\ -\frac{1}{r}F_2(r)\Omega_{\frac{3}{2}1m'}(\theta,\varphi)\end{pmatrix}. \tag{33}$$

The energy of the $2P_{1/2}$ state is

$$E_2=m_0c^2\sqrt{\tfrac{1}{2}(1+s_1)},\qquad s_1=\sqrt{1-Z^2\alpha^2}, \tag{34}$$

thus the emission frequency of the atomic transition $2P_{1/2}$ to $1S_{1/2}$ is given by

$$\omega_0^{(\mathrm{R})}=\frac{1}{\hbar}(E_2-E_1)=\frac{m_0c^2}{\hbar}\left[\sqrt{\frac{1}{2}(1+s_1)}-s_1\right]. \tag{35}$$

We choose by will $m'=\frac{1}{2}$; the possible (M,m) has two sets of values: $(M=0,m=\frac{1}{2})$ and $(M=1,m=-\frac{1}{2})$. The corresponding two coupling constants are calculated by equation (27) and are actually proportional to each other:

$$g_{k11(-1)}=-\sqrt{2}g_{k10(-1)}. \tag{36}$$

The resultant correlation spectrum may be shown as

$$R(\omega) = |B_0 B_0'|^2 Z^2\alpha^3 \frac{\omega}{2\pi}\left|S_0(\omega) + \frac{1}{3}S_0'(\omega) - \frac{2}{3}S_2'(\omega)\right|^2 \quad (37)$$

in which

$$S_0(\omega) = \frac{1}{\mathrm{i}k}\left[1 + \frac{Z\alpha}{\sqrt{\frac{1}{2}(1-s_1)}}\right]^{-s_1}\left[1 + \frac{\sqrt{\frac{1}{2}(1-s_1)}}{Z\alpha}\right]^{-s_1} \times \left\{\frac{1}{1-s_1}\frac{\Gamma(2s_1)}{(1-\mathrm{i}ka)^{2s_1}} + \frac{\sqrt{\frac{1}{2}(1-s_1)}}{Z\alpha(1-s_1)(1+2s_1)} \times \frac{\sqrt{2(1-s_1)} - 2Z\alpha}{\sqrt{\frac{1}{2}(1-s_1)} + Z\alpha}\frac{\Gamma(2s_1+1)}{(1-\mathrm{i}ka)^{2s_1+1}} - \text{c.c.}\right\}, \quad (38a)$$

$$S_0'(\omega) = -\frac{1}{\mathrm{i}k}\left[1 + \frac{Z\alpha}{\sqrt{\frac{1}{2}(1-s_1)}}\right]^{-s_1}\left[1 + \frac{\sqrt{\frac{1}{2}(1-s_1)}}{Z\alpha}\right]^{-s_1} \times \left\{\frac{1}{1+s_1}\frac{\Gamma(2s_1)}{(1-\mathrm{i}ka)^{2s_1}} + \frac{s_1\sqrt{2(1-s_1)} + Z\alpha}{\sqrt{\frac{1}{2}(1-s_1)} + Z\alpha} \times \frac{1}{Z^2\alpha^2(1+2s_1)}\frac{\Gamma(2s_1+1)}{(1-\mathrm{i}ka)^{2s_1+1}} - \text{c.c.}\right\}, \quad (38b)$$

$$S_2'(\omega) = -S_0'(\omega) + \frac{3}{k}\frac{1}{1+s_1}\frac{1}{(ka)^2}\left[1 + \frac{Z\alpha}{\sqrt{\frac{1}{2}(1-s_1)}}\right]^{-s_1} \times \left[1 + \frac{\sqrt{\frac{1}{2}(1-s_1)}}{Z\alpha}\right]^{-s_1}\left\{\frac{\mathrm{i}\Gamma(2s_1-2)}{(1-\mathrm{i}ka)^{2s_1-2}} + \left[\mathrm{i}\frac{s_1\sqrt{2(1-s_1)} + Z\alpha}{\sqrt{\frac{1}{2}(1-s_1)} + Z\alpha}\frac{1}{(1-s_1)(1+2s_1)} + ka\right] \times \frac{\Gamma(2s_1-1)}{(1-\mathrm{i}ka)^{2s_1-1}} + ka\frac{s_1\sqrt{2(1-s_1)} + Z\alpha}{\sqrt{\frac{1}{2}(1-s_1)} + Z\alpha} \times \frac{1}{(1-s_1)(1+2s_1)}\frac{\Gamma(2s_1)}{(1-\mathrm{i}ka)^{2s_1}} + \text{c.c.}\right\} \quad (38c)$$

with

$$a = \frac{a_B/Z}{1 + \frac{\sqrt{\frac{1}{2}(1-s_1)}}{Z\alpha}}, \quad (39)$$

which is different from the non-relativistic transition radius of 2P to 1S. Only when $Z\alpha \ll 1$ does equation (39) approach equation (32).

Before we go a further step, we make a check on the above derived $R(\omega)$ by investigation of their non-relativistic limit and compare them with those given in [9] and [10].

If Z is small so that $Z^2\alpha^2$ can be neglected as compared with unity, equations (30) and (37) should go over to the corresponding non-relativistic results.

For the atomic transition $2P_{3/2}$ to $1S_{1/2}$, when $\sqrt{1-Z^2\alpha^2}$ and $\sqrt{4-Z^2\alpha^2}$ are approximated by one and two respectively, we get from equation (30)

$$S_0(\omega) = \frac{8}{27}\frac{a(3-k^2a^2)}{(1+k^2a^2)^3}, \qquad S_2(\omega) = \frac{32}{27}\frac{k^2a^3}{(1+k^2a^2)^3}, \quad (40)$$

hence

$$R(\omega) = \frac{2^{10}}{3^9}Z^2\alpha^3\frac{\omega}{\pi(1+\frac{\omega^2a^2}{c^2})^4}\left[1 - \frac{3\frac{\omega^2a^2}{c^2}}{2(1+\frac{\omega^2a^2}{c^2})}\right]^2, \quad (41)$$

while the 'usual' non-relativistic result is (see, for example [6, 7, 10, 11])

$$R(\omega) = \frac{\gamma_A}{2\pi\omega_0}\frac{\omega}{(1+\frac{\omega^2a^2}{c^2})^4} = \frac{2^{10}}{3^9}Z^2\alpha^3\frac{\omega}{\pi(1+\frac{\omega^2a^2}{c^2})^4}, \quad (42a)$$

in which γ_A is the Einstein A coefficient, given by

$$\gamma_A = \left(\frac{4}{9}\right)^4 Z^4\alpha^5\frac{m_0c^2}{\hbar}. \quad (42b)$$

We see there is an additional correction factor $[1 - 3\frac{\omega^2a^2}{c^2}/2(1+\frac{\omega^2a^2}{c^2})]^2$ in equation (41) as compared with equation (42*a*), which makes $R(\omega)$ have a zero point at $\omega a/c = \sqrt{2}$. We will see that this additional factor comes from the interaction of the electron spin-magnet with the magnetic field **B** of the emitted light. This interaction is not included in the non-relativistic electric-dipole emission, while it does contribute in the present formulation. The reason lies in the fact that in the 'usual' non-relativistic theory the electric-dipole emission is connected to the atomic electric-dipole moment, while in the present formulation it is defined by the angular momentum and parity of the emitted photon to be $(1, -1)$. The electron spin has no contribution to the former, but does contribute in the latter.

The situation for atomic $2P_{1/2}$ to $1S_{1/2}$ is similar. In this case, the non-relativistic limits of $1 - s_1$ and $\frac{Z\alpha}{\sqrt{\frac{1}{2}(1-s_1)}}$ are $\frac{1}{2}Z^2\alpha^2$ and 2 respectively, hence to the leading power of $Z\alpha$, $S_0(\omega)$, $S_0'(\omega)$ and $S_2'(\omega)$ are given by

$$S_0(\omega) = \frac{32}{81}\frac{1}{Z^2\alpha^2}\frac{a(3+5k^2a^2)}{(1+k^2a^2)^3}, \qquad S_0'(\omega) = -\frac{32}{81}\frac{1}{Z^2\alpha^2}\frac{a(3-k^2a^2)}{(1+k^2a^2)^3}, \qquad S_2'(\omega) = -\frac{128}{81}\frac{a}{Z^2\alpha^2}\frac{k^2a^2}{(1+k^2a^2)^3}, \quad (43)$$

in which a is reduced to that given by equation (32), so its value becomes the same as in $2P_{3/2}$ to $1S_{1/2}$. The coefficient $|B_0B_0'|^2$ is reduced to $(4\frac{Z}{a_B})(\frac{3}{32}Z^4\alpha^4\frac{Z}{a_B})$, hence the resultant correlation spectrum is approximated by

$$R(\omega) = \frac{2^{10}}{3^9}Z^2\alpha^3\frac{\omega}{\pi}\frac{(1+4k^2a^2)^2}{(1+k^2a^2)^6} = \frac{2^{10}}{3^9}Z^2\alpha^3\frac{\omega}{\pi}\frac{1}{(1+\frac{\omega^2a^2}{c^2})^4}\left(1 + \frac{3\frac{\omega^2a^2}{c^2}}{1+\frac{\omega^2a^2}{c^2}}\right)^2. \quad (44)$$

Compared with the 'usual' non-relativistic result equation (42), the present additional correction factor is $[1+3\frac{\omega^2a^2}{c^2}/(1+\frac{\omega^2a^2}{c^2})]^2$.

Equations (44) and (41) show explicitly the large differences between these two correlation spectra in the high frequency region: the latter has a zero point at $\frac{\omega^2a^2}{c^2}=2$ and is 1/64 of the former for $\frac{\omega^2a^2}{c^2}\gg 1$.

Now we come to show that these additional correction factors indeed stem from spin–B coupling.

The corresponding non-relativistic interaction Hamiltonian for this coupling is given by

$$\hat{H}'_{\rm int}=\frac{e\hbar}{2mc}\int\hat{\varphi}^{+}(\mathbf{x})\sigma\hat{\varphi}(\mathbf{x})\cdot\hat{\mathbf{B}}(\mathbf{x})\,\mathrm{d}\tau \tag{45}$$

which will contribute an extra coupling constant $g'_{k1M(-1)}$ given by

$$g'_{k1M(-1)}=\frac{1}{\mathrm{i}\hbar}\int\varphi_2^{+}(\mathbf{x})\sigma\varphi_1(\mathbf{x})\cdot\mathbf{B}_{k1M(-1)}(\mathbf{x})\,\mathrm{d}\tau. \tag{46}$$

We note in passing that $\frac{e\hbar}{2m_0c}\sigma\cdot\mathbf{B}$ coupling also belongs to the $-\frac{1}{c}\mathbf{j}\cdot\mathbf{A}$ type of interaction even in non-relativistic theory, because $\mathbf{j}$ actually consists of two parts: the translational current and spin-magnetic current. The translational current density $\hat{j}_{\rm T}=\frac{i\hbar e}{m_0}\hat{\varphi}\nabla\hat{\varphi}$, and the spin-magnetic current density $\hat{j}_M=-\frac{e\hbar}{2m_0}\nabla\times(\hat{\varphi}\sigma\hat{\varphi})$. The former leads to $\frac{e}{m_0c}\mathbf{P}\cdot\mathbf{A}$ coupling; the latter contributes a term $-\frac{1}{c}\int\hat{j}_M\cdot\hat{\mathbf{A}}\,\mathrm{d}^3x$, which after integration by parts just transforms to equation (45).

Since in some literature [8] the factor $[1+3\frac{\omega^2a^2}{c^2}/(1+\frac{\omega^2a^2}{c^2})]^2=[(1+4\frac{\omega^2a^2}{c^2})/(1+\frac{\omega^2a^2}{c^2})]^2$ in equation (44) is referred to relativistic correction, we will derive the non-relativistic $g'_{k1M(-1)}$ to verify our assertion stated before (equations (45) and (46)).

(i) *Transition* $2P_{3/2}$ *to* $1S_{1/2}$. The initial state of the atom is still $(j',m')=(\frac{3}{2},\frac{3}{2})$. As mentioned below equation (28), the allowed value of (M,m), the third component of the total angular momentum of the photon and final state of the atom respectively, is just $(1,\frac{1}{2})$. This means only $g'_{k11(-1)}$ is nonzero. Substituting the non-relativistic atomic wavefunctions

$$\varphi_2(\mathbf{x})=\begin{pmatrix}R_2(r)Y_{11}(\theta,\varphi)\\0\end{pmatrix}, \tag{47a}$$

$$\varphi_1(\mathbf{x})=\begin{pmatrix}R_1(r)Y_{10}(\theta,\varphi)\\0\end{pmatrix}, \tag{47b}$$

and magnetic field intensity

$$\mathbf{B}_{k11(-1)}=\mathrm{i}\sqrt{\frac{2\pi\hbar\omega^3}{c^2R_0}}g_1(kr)[Y_{10}(\theta,\varphi)\mathbf{n}^{(+1)}-Y_{11}(\theta,\varphi)\mathbf{n}^{(0)}] \tag{48}$$

into equation (50), and carrying out the space integration, we get

$$g'_{k11(-1)}=-eZ\alpha\left(\frac{2}{3}\right)^4\sqrt{\frac{3\omega}{\hbar R_0}}\frac{\frac{\omega^2a^2}{c^2}}{(1+\frac{\omega^2a^2}{c^2})^3}. \tag{49}$$

The original non-relativistic coupling constant $g_{k11(-1)}$ can be shown as

$$g_{k11(-1)}=eZ\alpha\left(\frac{2}{3}\right)^5\sqrt{\frac{3\omega}{\hbar R_0}}\frac{1}{(1+\frac{\omega^2a^2}{c^2})^2}. \tag{50}$$

We see $g'_{k11(-1)}$ is of order $[\frac{\omega^2a^2}{c^2}/(1+\frac{\omega^2a^2}{c^2})]g_{k11(-1)}$, hence is small in the low frequency range.

The total coupling constant for the transition $2P_{3/2}$ to $1S_{1/2}$ with the emitted photon of mode $(k11(-1))$ is then given by

$$g_{k11(-1)}+g'_{k11(-1)}=eZ\alpha\left(\frac{2}{3}\right)^5\sqrt{\frac{3\omega}{\hbar R_0}}\frac{1-\frac{1}{2}\frac{\omega^2a^2}{c^2}}{(1+\frac{\omega^2a^2}{c^2})^3}, \tag{51}$$

and the corresponding correlation spectrum is

$$\begin{aligned}R(\omega)&=\frac{R_0}{c\pi}|g_{k11(-1)}+g'_{k11(-1)}|^2\\&=\frac{2^{10}}{3^9}Z^2\alpha^3\frac{\omega}{\pi(1+\frac{\omega^2a^2}{c^2})^4}\left[1-\frac{3\frac{\omega^2a^2}{c^2}}{2(1+\frac{\omega^2a^2}{c^2})}\right]^2,\end{aligned} \tag{52}$$

identical to that of equation (41).

(ii) *Transition* $2P_{1/2}$ *to* $1S_{1/2}$. The quantum number (j',m') for the initial atomic state is taken as before: $(\frac{1}{2},\frac{1}{2})$. Now there are two possible final atomic states: $(j,m)=(\frac{1}{2},\frac{1}{2})$ and $(\frac{1}{2},-\frac{1}{2})$, with corresponding photon quantum numbers $(k10(-1))$ and $(k11(-1))$ respectively.

The non-relativistic wavefunction of the initial atomic state is

$$\varphi_2(\mathbf{x})=R_2(r)\begin{pmatrix}-\frac{1}{\sqrt{3}}Y_{10}(\theta,\varphi)\\\sqrt{\frac{2}{3}}Y_{11}(\theta,\varphi)\end{pmatrix}, \tag{53}$$

and the two possible final states are given by

$$\varphi_1(\mathbf{x})=\begin{pmatrix}R_1(r)Y_{00}(\theta,\varphi)\\0\end{pmatrix},\qquad\begin{pmatrix}0\\R_1(r)Y_{00}(\theta,\varphi)\end{pmatrix}. \tag{54}$$

The relevant magnetic field intensities are $\mathbf{B}_{k10(-1)}$ and $\mathbf{B}_{k11(-1)}$ respectively. The expression for the latter has already been given by equation (48); the former has the expression

$$\begin{aligned}\mathbf{B}_{k10(-1)}=\mathrm{i}\sqrt{\frac{2\pi\hbar\omega^3}{c^2R_0}}g_1(kr)[&Y_{1-1}(\theta,\varphi)\mathbf{n}^{(+1)}\\&-Y_{11}(\theta,\varphi)\mathbf{n}^{(-1)}].\end{aligned} \tag{55}$$

The two magnetic coupling constants can be calculated according to equation (46) with the result

$$\begin{aligned}g'_{k10(-1)}&=-eZ\alpha\left(\frac{2}{3}\right)^5\sqrt{\frac{\omega}{\hbar R_0}}\frac{3\frac{\omega^2a^2}{c^2}}{(1+\frac{\omega^2a^2}{c^2})^3},\\g'_{k11(-1)}&=eZ\alpha\left(\frac{2}{3}\right)^4\sqrt{\frac{8\omega}{\hbar R_0}}\frac{\frac{\omega^2a^2}{c^2}}{(1+\frac{\omega^2a^2}{c^2})^3}.\end{aligned} \tag{56}$$

We should add them to the $g_{k10(-1)}$ and $g_{k11(-1)}$ respectively. But from the 'usual' non-relativistic spectrum equation (42), which also applies to the case $2P_{1/2}$ to $1S_{1/2}$, we cannot derive the individual values of $g_{k10(-1)}$ and $g_{k11(-1)}$. Their values should be calculated by the non-relativistic $\mathbf{P}\cdot\mathbf{A}$ interaction Hamiltonian. The corresponding formulae are

$$g_{kJMP}=-\frac{e}{m_0c}\int\varphi_2^{+}(\mathbf{x})\nabla\varphi_1(\mathbf{x})\cdot\mathbf{A}_{kJMP}(\mathbf{x})\,\mathrm{d}^3x. \tag{57}$$

The results so obtained are given by

$$\begin{aligned}g_{k10(-1)}&=-eZ\alpha\left(\frac{2}{3}\right)^5\sqrt{\frac{\omega}{\hbar R_0}}\frac{1}{(1+\frac{\omega^2a^2}{c^2})^2},\\g_{k11(-1)}&=eZ\alpha\left(\frac{2}{3}\right)^5\sqrt{\frac{2\omega}{\hbar R_0}}\frac{1}{(1+\frac{\omega^2a^2}{c^2})^2}.\end{aligned} \tag{58}$$

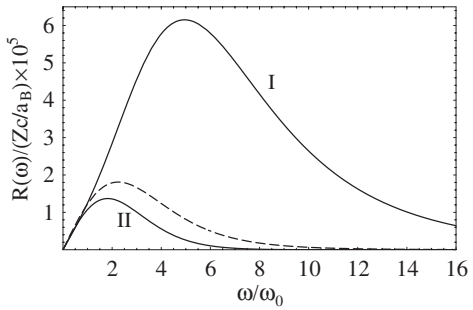

Figure 1. The relativistic correlation spectra $R(\omega)$ of electric-dipole emission. (I) For transition $2P_{1/2}$ to $1S_{1/2}$, $Z = 92$. (II) For transition $2P_{3/2}$ to $1S_{1/2}$, $Z = 92$. Dashed curve—the 'usual' non-relativistic correlation spectrum 2P to 1S, $Z = 92$.

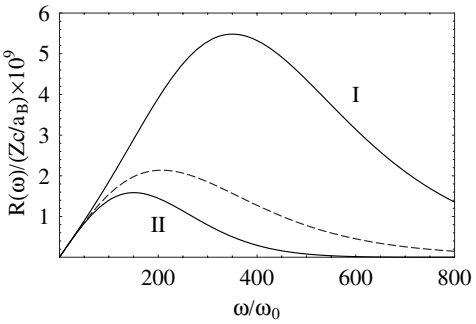

Figure 2. The non-relativistic correlation spectra $R(\omega)$ of electric-dipole emission with spin magnet–**B** coupling included. (I) For transition $2P_{1/2}$ to $1S_{1/2}$, $Z = 1$. (II) For transition $2P_{3/2}$ to $1S_{1/2}$, $Z = 1$. Dashed curve—the 'usual' non-relativistic correlation spectrum 2P to 1S, $Z = 1$.

It is easy to check that $\frac{R_0}{c\pi}[|g_{k10(-1)}|^2 + |g_{k11(-1)}|^2]$ indeed leads to equation (42*a*).

The two total coupling constants are the sum of equations (56) and (58), with the result

$$\begin{aligned} &g_{k10(-1)} + g'_{k10(-1)} \\ &= -eZ\alpha\left(\frac{2}{3}\right)^5\sqrt{\frac{\omega}{\hbar R_0}}\frac{1}{(1+\frac{\omega^2a^2}{c^2})^2}\left(1+\frac{3\frac{\omega^2a^2}{c^2}}{1+\frac{\omega^2a^2}{c^2}}\right), \\ &g_{k11(-1)} + g'_{k11(-1)} \\ &= eZ\alpha\left(\frac{2}{3}\right)^5\sqrt{\frac{2\omega}{\hbar R_0}}\frac{1}{(1+\frac{\omega^2a^2}{c^2})^2}\left(1+\frac{3\frac{\omega^2a^2}{c^2}}{1+\frac{\omega^2a^2}{c^2}}\right). \end{aligned} \tag{59}$$

Therefore, we arrive at

$$\begin{aligned} R(\omega) &= \frac{R_0}{c\pi}[|g_{k10(-1)} + g'_{k10(-1)}|^2 + |g_{k11(-1)} + g'_{k11(-1)}|^2] \\ &= \frac{2^{10}}{3^9}Z^2\alpha^3\frac{\omega}{\pi}\frac{1}{(1+\frac{\omega^2a^2}{c^2})^4}\left(1+\frac{3\frac{\omega^2a^2}{c^2}}{1+\frac{\omega^2a^2}{c^2}}\right)^2, \end{aligned} \tag{60}$$

identical to equation (44).

The above investigation justifies our assertion that the two additional correction factors indeed come from the spin interaction term in the non-relativistic $\hat{H}_{\rm int}$. It is not the relativistic correction claimed by Seke [8]. The true relativistic corrections are higher order terms of α (or $Z\alpha$), which are neglected by Seke.

4. The numerical results of electric-dipole emission

The largest value of Z for stable nuclei is 92. In figure 1 we plot the relativistic correlation spectra $R(\omega)$ for transitions $2P_{3/2}$ to $1S_{1/2}$ and $2P_{1/2}$ to $1S_{1/2}$ of a hydrogen-like atom with this value of Z, and compare them with the 'usual' non-relativistic correlation spectrum. The abscissa is taken as ω/ω_0, with ω_0 denoting the corresponding non-relativistic value which is the same for both $2P_{3/2}$ to $1S_{1/2}$ and $2P_{1/2}$ to $1S_{1/2}$ transitions:

$$\omega_0 = \frac{3}{8}Z^2\alpha\left(\frac{c}{a_B}\right). \tag{61}$$

The ordinate is taken as $R(\omega)/(\frac{Zc}{a_B})$, which is also dimensionless. We note that $\omega_0^{(\rm R)}$ is different from ω_0 quite obviously for large Z. For $Z = 92$,

$$\begin{aligned} \omega_0^{(\rm R)}(2P_{3/2} \to 1S_{1/2}) &\simeq 1.19\omega_0, \\ \omega_0^{(\rm R)}(2P_{1/2} \to 1S_{1/2}) &\simeq 1.14\omega_0. \end{aligned} \tag{62}$$

It can be shown that $R(\omega)$ spreads over a range of several hundred ω_0 for $Z = 1$ (cf figure 2) and shrinks to several or a dozen ω_0 for $Z = 92$. For non-relativistic spectra, this shrinking effect can be shown quantitatively by equations (41), (42*a*) and (44) and by

$$\frac{\omega a}{c} = \frac{1}{4}Z\alpha\left(\frac{\omega}{\omega_0}\right),$$

since these spectra are of the form

$$R(\omega) = \frac{2^9}{3^8}\frac{c}{\pi a_B}Z^3\alpha^3 f\left(\frac{1}{4}Z\alpha\frac{\omega}{\omega_0}\right),$$

which means the spread range of $R(\omega)$ on the abscissa $\frac{\omega}{\omega_0}$ is inversely proportional to Z.

We have pointed out that there is a zero point $\omega = \sqrt{2}c/a = \frac{4\sqrt{2}}{Z\alpha}\omega_0$ in the tail-part of the non-relativistic correlation spectrum for the $2P_{3/2}$ to $1S_{1/2}$ transition. This zero point still exists in the relativistic $R(\omega)$, but its position moves to $(\sim\frac{8}{Z\alpha}\omega_0)$. This means it is not necessary for $R(\omega)$ to have just one peak (however, the second peak is too small to be seen in figure 1).

In figure 2, we compare the 'usual' non-relativistic $R(\omega)$ given by equation (42*a*) with those in which the spin magnet–**B** coupling is included (namely equations (41) and (44)). The value of Z is taken as unity, hence corresponding to the hydrogen atom. We see even in this smallest value of Z, the magnetic interaction contributes significantly to $R(\omega)$ in the high frequency region. We note in passing that for $Z = 1$ equations (41) and (44) almost coincide with the corresponding relativistic spectra.

The situation for $Z = 50$ is similar to the case of $Z = 92$ but the coincident part of the three curves in the low frequency region becomes larger (see figure 3). Figure 3 also shows explicitly how the spread range of $R(\omega)$ over ω/ω_0 changes as compared with that of $Z = 92$.

The correlation function $U(\tau)$ may be expressed by

$$U(\tau) = F(\tau)e^{i\omega_0^{(\rm R)}\tau}, \tag{63}$$

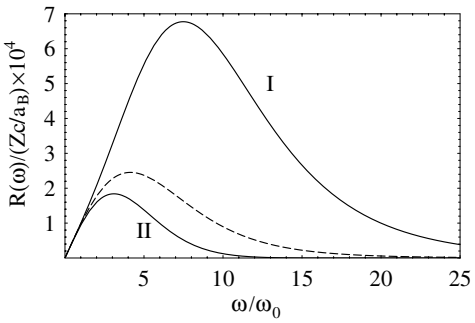

Figure 3. The relativistic correlation spectra $R(\omega)$ of electric-dipole emission. (I) For transition $2P_{1/2}$ to $1S_{1/2}$, $Z = 50$. (II) For transition $2P_{3/2}$ to $1S_{1/2}$, $Z = 50$. Dashed curve—the 'usual' non-relativistic correlation spectrum 2P to 1S, $Z = 50$.

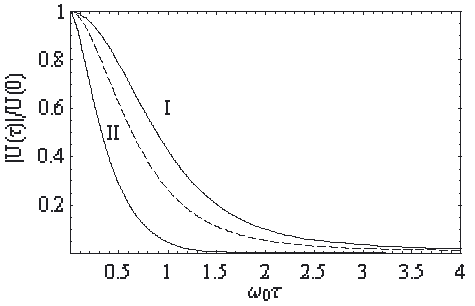

Figure 4. The relativistic correlation function $U(\tau)$ of electric-dipole emission: the absolute value. (I) For transition $2P_{3/2}$ to $1S_{1/2}$, $Z = 92$, $U(0) = 1.80 \times 10^{-4}\omega_0^2$. (II) For transition $2P_{1/2}$ to $1S_{1/2}$, $Z = 92$, $U(0) = 2.08 \times 10^{-3}\omega_0^2$. Dashed curve—the 'usual' non-relativistic correlation spectrum 2P to 1S, $Z = 92$, $U(0) = 3.22 \times 10^{-4}\omega_0^2$.

in which $F(\tau)$ is the conventional Fourier transform of $R(\omega)$:

$$F(\tau) = \int_0^\infty R(\omega)\mathrm{e}^{\mathrm{i}\omega\tau}\,\mathrm{d}\omega. \tag{64}$$

The numerically calculated results of correlation function are shown in figures 4–7. Figure 4 shows the absolute value of $U(\tau)/U(0)$ for $Z = 92$. We see that the differences between the relativistic curves and the 'usual' non-relativistic curves, as well as the differences between the corresponding $U(0)$, are quite significant. The widths τ_W at half height of $|U(\tau)|/U(0)$ for $2P_{3/2}$ to $1S_{1/2}$ and $2P_{1/2}$ to $1S_{1/2}$ are $0.885/\omega_0 = 1.05/\omega_0^{(R)}$ and $0.321/\omega_0 = 0.364/\omega_0^{(R)}$ respectively. The corresponding ratios of τ_W to τ_A (where $\tau_A = 1/\gamma_A$ is the Weisskopf–Wigner decay time) are equal to 3.03×10^{-4} and 1.10×10^{-4}, being quite small quantities.

The curves of $\theta_U(\tau)$, the arg $U(\tau)$, are shown in figure 5 for $Z = 92$. The curve for $2P_{3/2}$ to $1S_{1/2}$ is flatter than that for $2P_{1/2}$ to $1S_{1/2}$. They become straight lines when $\omega_0\tau \gtrsim 2$. For comparison, the argument of the 'usual' non-relativistic correlation function is also plotted.

Figure 6 shows $|U(\tau)|/U(0)$ for $Z = 50$. The widths at half height τ_W measured by $1/\omega_0$ become smaller than those for $Z = 92$. Their values are reduced to $0.539/\omega_0$ and $0.237/\omega_0$ respectively. Hence the usual saying that τ_W is about $1/\omega_0$ is not so precise.

Figure 7 expresses the corresponding $\theta_U(\tau)$ for $Z = 50$.

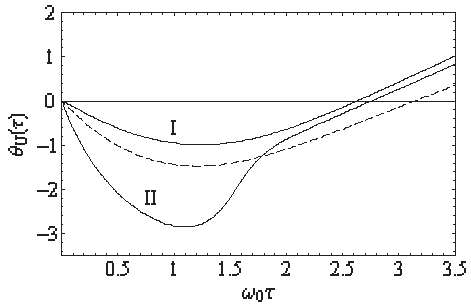

Figure 5. The relativistic correlation function $U(\tau)$ of electric-dipole emission: θ_U (the argument of U). (I) For transition $2P_{3/2}$ to $1S_{1/2}$, $Z = 92$. (II) For transition $2P_{1/2}$ to $1S_{1/2}$, $Z = 92$. Dashed curve—the 'usual' non-relativistic correlation spectrum 2P to 1S, $Z = 92$.

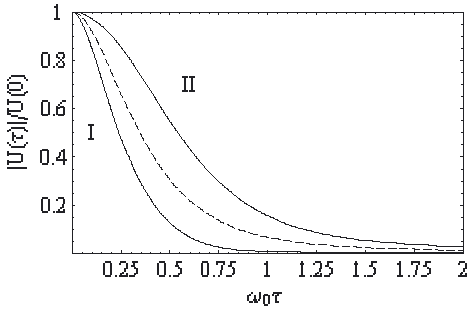

Figure 6. The relativistic correlation function $U(\tau)$ of electric-dipole emission: the absolute value. (I) For transition $2P_{3/2}$ to $1S_{1/2}$, $Z = 50$, $U(0) = 1.60 \times 10^{-4}\omega_0^2$. (II) For transition $2P_{1/2}$ to $1S_{1/2}$, $Z = 50$, $U(0) = 1.28 \times 10^{-3}\omega_0^2$. Dashed curve—the 'usual' non-relativistic correlation spectrum 2P to 1S, $Z = 50$, $U(0) = 3.22 \times 10^{-4}\omega_0^2$.

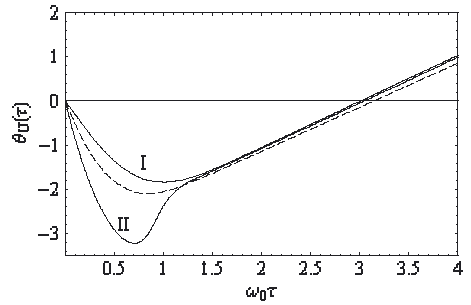

Figure 7. The relativistic correlation function $U(\tau)$ of electric-dipole emission: θ_U (the argument of U). (I) For transition $2P_{3/2}$ to $1S_{1/2}$, $Z = 50$. (II) For transition $2P_{1/2}$ to $1S_{1/2}$, $Z = 50$. Dashed curve—the 'usual' non-relativistic correlation spectrum 2P to 1S, $Z = 50$.

Having obtained the correlation function $U(\tau)$, we proceed to solve the integro-differential equation equation (11) numerically as in [10], but with higher accuracy (the average error is less than 0.1%), and hence the present results will be more reliable. The obtained results on the evolution of the upper level population $N_2(t)$ will be compared with the 'usual' non-relativistic results (calculated also by equations (11) and (13) but making use of equation (42*a*)) as well as with Weisskopf–Wigner results.

We plot the decay curves of N_2 for both $2P_{3/2}$ to $1S_{1/2}$ and $2P_{1/2}$ to $1S_{1/2}$ processes for $Z = 92$ in figure 8. The abscissa is

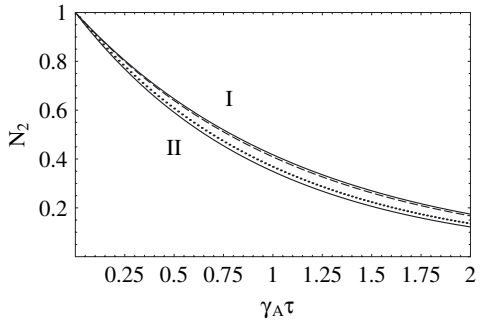

Figure 8. The decay of upper level population N_2. (I) For transition $2P_{3/2}$ to $1S_{1/2}$, $Z = 92$. (II) For transition $2P_{1/2}$ to $1S_{1/2}$, $Z = 92$. Dashed curve—the 'usual' non-relativistic result for 2P to 1S, $Z = 92$. Dotted curve—the Wigner–Weisskopf result for 2P to 1S (non-relativistic, neglecting the finite dimension of the atom as compared with the photon wavelength), $Z = 92$.

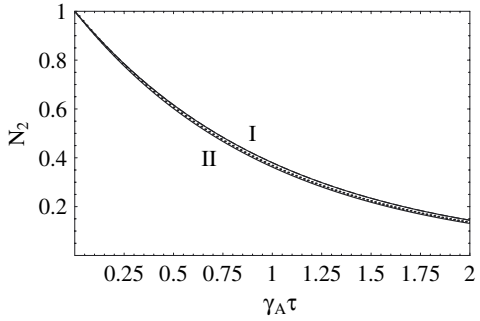

Figure 9. The decay of upper level population N_2. (I) For transition $2P_{3/2}$ to $1S_{1/2}$, $Z = 50$. (II) For transition $2P_{1/2}$ to $1S_{1/2}$, $Z = 50$. Dashed curve—the 'usual' non-relativistic result for 2P to 1S, $Z = 50$. Dotted curve—the Wigner–Weisskopf result for 2P to 1S (non-relativistic, neglecting the finite dimension of the atom as compared with the photon wavelength), $Z = 50$ (this curve almost coincides with curve I).

taken as $\gamma_A\tau$, where γ_A is given by equation (42*b*). We see that the former is slightly above the 'usual' non-relativistic curve, while the latter is somewhat below the Weisskopf–Wigner result.

We have noted [9, 10] that the difference between the 'usual' non-relativistic result and the Weisskopf–Wigner result lies in the fact that the latter has neglected the finite size of the electric dipole as compared with the emitted photon wavelength and has made the Markovian approximation. Actually, the first factor makes the main effect. Figure 8 shows that the difference between these two curves is quite large. But the difference between the curves of relativistic $2P_{3/2}$ to $1S_{1/2}$ and $2P_{1/2}$ to $1S_{1/2}$ is even larger.

The relativistic decay curves under the Markovian approximation are also calculated, which are expressed by

$$N_2(t) = \mathrm{e}^{-\gamma t} \tag{65a}$$

with the relativistic decay rate γ given by equation (17). For $Z = 92$, its value is given by

$$\gamma = \begin{cases} 0.873\gamma_A, & \text{for } 2P_{3/2} \text{ to } 1S_{1/2}, \\ 1.052\gamma_A, & \text{for } 2P_{1/2} \text{ to } 1S_{1/2}. \end{cases} \tag{65b}$$

It may be compared with the non-relativistic values given by equations (41) and (44) for $Z = 92$:

$$\gamma = \begin{cases} 0.823\gamma_A, & \text{for } 2P_{3/2} \text{ to } 1S_{1/2}, \\ 1.048\gamma_A, & \text{for } 2P_{1/2} \text{ to } 1S_{1/2}. \end{cases} \tag{65c}$$

We see the relativistic corrections are about 6% and 0.4%.

The Z dependence of the relativistic γ is rather complicated, but for the 'usual' non-relativistic γ its Z dependence is rather simple, since according to equation (42*a*) and $\frac{\omega_0 a}{c} = \frac{1}{4}Z\alpha$ with $\omega_0 = \frac{3}{8}\frac{c}{a_B}Z^2\alpha$, it is equal to $(\frac{2}{3})^8\frac{c}{a_B}[Z^4\alpha^4/(1+\frac{1}{16}Z^2\alpha^2)^4]$. We see that it basically increases with Z as Z^4.

We note in passing that the two transitions ($2P_{3/2}$ to $1S_{1/2}$ and $2P_{1/2}$ to $1S_{1/2}$) not only have different spectrum functions $R(\omega)$, but also have different $\omega_0^{(R)}$, as shown in equation (62). The value of γ is determined by both factors.

When we compare the Markovian curves with γ of equation (65*b*) for $Z = 92$ with those relativistic (non-Markovian) curves plotted in figure 8, we find that their differences are very small, even undifferentiated when plotted in the same figure. This means the Markovian approximation works quite well in the main period of decay even for the largest realistic atomic number Z.

The above results are not out of expectation. It is known that $\delta(\tau)$ can be expressed by alternative limiting forms such as $\frac{1}{\pi}\lim_{\epsilon\to 0}\frac{\epsilon}{\tau^2+\epsilon^2}$ and $\frac{1}{\pi}\lim_{\omega\to\infty}\frac{\sin\omega\tau}{\tau}$. The former has typical peaked form with infinitesimal width ϵ, and the latter oscillates with infinite frequency for $\tau > 0$. Now the relativistic correlation functions $U(\tau)$ calculated above have both the peaked form and oscillating behaviour outside the peak region. The oscillation frequencies are $\omega_0^{(R)}$, and the peak widths τ_W are of order $1/\omega_0^{(R)}$ or even smaller as shown before. Since $1/\omega_0^{(R)}$ compared with the decay time $1/\gamma$ is of order 10^{-4}, it is reasonable that Markovian approximation turns out to be a quite good approximation in practical use.

The calculated results for $Z = 50$ are plotted in figure 9. The relativistic curve for $2P_{3/2}$ to $1S_{1/2}$ is just below the 'usual' non-relativistic curve and almost undifferentiated with it. The difference between the relativistic curve for $2P_{1/2}$ to $1S_{1/2}$ and Weisskopf–Wigner curve also becomes smaller than that of $Z = 92$.

We show in passing the effect of spin magnet–**B** interaction on the non-relativistic atom decay behaviour, which is neglected in the 'usual' non-relativistic theory. In the case up to $Z = 10$ this correction can be neglected, but when Z increases to 50 the correction becomes perceivable (see figure 10); the curve with spin magnet–**B** interaction almost coincides with the relativistic curve for the transition $2P_{1/2}$ to $1S_{1/2}$, and in the case of $2P_{3/2}$ to $1S_{1/2}$ transition, the difference between it and the 'usual' non-relativistic result even becomes larger than the relativistic correction.

The situation for $Z = 92$ is similar, but the differences increase as can be seen from figure 11.

5. Brief summary and discussion

The multipole em field formulation is used to study the relativistic correction and non-Markovian correction

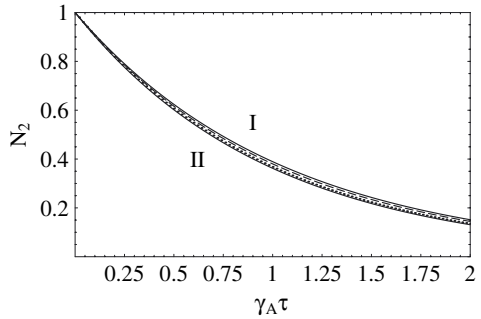

Figure 10. The non-relativistic decay of upper level population N_2 with spin magnet–**B** coupling included. (I) For transition $2P_{3/2}$ to $1S_{1/2}$, $Z = 50$. (II) For transition $2P_{1/2}$ to $1S_{1/2}$, $Z = 50$. Dashed curve—the 'usual' non-relativistic result for 2P to 1S (without spin interaction), $Z = 50$. Dotted curve—the Wigner–Weisskopf result (non-relativistic, neglecting the finite dimension of the atom as compared with the photon wavelength) without spin interaction, $Z = 50$.

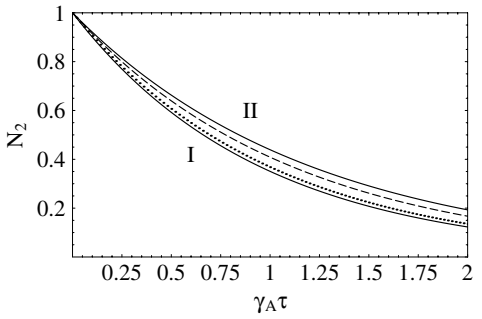

Figure 11. The non-relativistic decay of upper level population N_2 with spin magnet–**B** coupling included. (I) For transition $2P_{3/2}$ to $1S_{1/2}$, $Z = 92$. (II) For transition $2P_{1/2}$ to $1S_{1/2}$, $Z = 92$. Dashed curve—the 'usual' non-relativistic result for 2P to 1S (without spin interaction), $Z = 92$. Dotted curve—the Wigner–Weisskopf result (non-relativistic, neglecting the finite dimension of the atom as compared with the photon wavelength) without spin interaction, $Z = 92$.

of electric-dipole emission. The difference between this formulation (when used in the non-relativistic case) and the 'usual' non-relativistic formulation lies in the fact that the electron spin current contribution is fully included.

The relativistic correlation spectra $R(\omega)$ are first analytically derived, then the corresponding correlation functions $U(\tau)$ are numerically calculated. The absolute value of $U(\tau)$ is peaked at $\tau = 0$ and has a width of the order of $1/\omega_0^{(\mathrm{R})}$ or somewhat smaller. Outside the peak region, $U(\tau)$ oscillates with the frequency $\omega_0^{(\mathrm{R})}$, which will further cause the $U(\tau)$ outside the peak region effectively to die away. These two factors together make $U(\tau)$ approximate the δ-function when it is applied to functions with variation rate much smaller than $\omega_0^{(\mathrm{R})}$. In our investigated problems the condition of Markovian approximation for the main period of decay may be given roughly by

$$\frac{\gamma}{\omega_0^{(\mathrm{R})}} \ll 1$$

where γ is the relativistic decay coefficient, defined by the relativistic correlation spectrum $R(\omega^{(\mathrm{R})})$ as

$$\gamma = 2\pi R(\omega_0^{(\mathrm{R})}).$$

The present calculation shows that the non-Markovian correction is almost negligible in the main period of hydrogen-like atom spontaneous decay up to $Z = 92$, the largest value for stable nuclei. But the relativistic correction and finite atom-size correction to decay rate are quite evident for large Z.

We note that the corrections are j-dependent; when the initial atomic state changes from $2P_{3/2}$ to $2P_{1/2}$, the correction even changes sign.

Our numerical calculation is limited in the main period of decay. Besides the very beginning period $t < \tau_c$, which is negligibly small, in the remote tail of decay equation (15) may be also invalid; $\frac{\mathrm{d}}{\mathrm{d}t}C_2(t)$ may become not proportional to $C_2(t)$. If we write equation (11) as

$$\frac{\mathrm{d}}{\mathrm{d}t}C_2(t) = -\int_{t-\tau_c}^{t} U(t-t')C_2(t')\,\mathrm{d}t' - \int_0^{t-\tau_c} U(t-t')C_2(t')\,\mathrm{d}t' \tag{66}$$

where τ_c is the correlation interval of order $1/\omega_0$, the first part on the right-hand side gives the Markovian result, and the second term represents the non-Markovian correction. For very large values of t, the second term may become notable, because its integration interval becomes large while the value of $C_2(t')$ in the first term becomes small. To give a rough estimate of the non-Markovian correction, we approximate the $C_2(t')$ in the second term on the right-hand side by $\mathrm{e}^{-\beta_c t}$, so equation (66) turns out to be

$$\frac{\mathrm{d}}{\mathrm{d}t}C_2(t) = -\beta_c C_2(t) - F(t), \tag{67}$$

in which

$$F(t) \equiv \int_0^{t-\tau_c} U(t-t')\mathrm{e}^{-\beta_c t'}\,\mathrm{d}t' = \int_0^{\infty} \frac{R(\omega)}{\mathrm{i}(\omega-\omega_0^{(\mathrm{R})})-\beta_c} \times [\mathrm{e}^{-\mathrm{i}(\omega-\omega_0^{(\mathrm{R})})\tau_c+\beta_c(\tau_c-t)} - \mathrm{e}^{-\mathrm{i}(\omega-\omega_0^{(\mathrm{R})})t}]\,\mathrm{d}\omega. \tag{68}$$

The equation (67) is easily solved, with the result

$$C_2(t) = \mathrm{e}^{-\beta_c t}S(t), \tag{69}$$

$$S(t) = 1 - \int_0^t \mathrm{e}^{\beta_c t'}F(t')\,\mathrm{d}t'. \tag{70}$$

Substituting equation (70) into (69), we finally get

$$C_2(t) = \mathrm{e}^{-\beta_c t}[1-\Delta(t)], \tag{71}$$

with

$$\Delta(t) = \int_0^{\infty} \frac{R(\omega)}{\mathrm{i}(\omega-\omega_0^{(\mathrm{R})})-\beta_c}\left[\mathrm{e}^{-\mathrm{i}(\omega-\omega_0^{(\mathrm{R})})\tau_c+\beta_c\tau_c}t + \frac{1}{\mathrm{i}(\omega-\omega_0^{(\mathrm{R})})-\beta_c}(\mathrm{e}^{-\mathrm{i}(\omega-\omega_0^{(\mathrm{R})})t+\beta_c t}-1)\right]\mathrm{d}\omega, \tag{72}$$

which is supposed to measure the percentage of the non-Markovian correction.

We have calculated $\Delta(t)$ in the range from $t = 0$ (except the very beginning) to $t = 5/\gamma_A$ for $Z = 92$. The value of β_c is taken as $(0.436\text{–}0.207\mathrm{i})\gamma_A$ for $2P_{3/2} \to 1S_{1/2}$, and

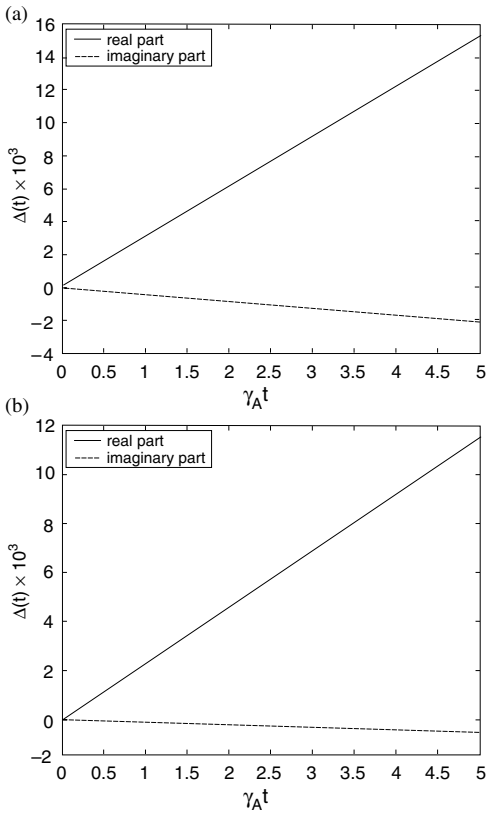

Figure 12. (a) The non-Markovian correction $\Delta(t)$ for process $2P_{3/2} \rightarrow 1S_{1/2}$, $Z = 92$. (b) The non-Markovian correction $\Delta(t)$ for process $2P_{1/2} \rightarrow 1S_{1/2}$, $Z = 92$.

$(0.524–1.65i)\gamma_A$ for $2P_{1/2} \rightarrow 1S_{1/2}$. The numerical values of $\Delta(t)$ so obtained are roughly represented by figure 12. From these figures we see that $\Delta(t)$, the non-Markovian correction, is small but non-zero, and is nearly proportional to t in this range. Since $\Delta(t)$ is small, when it is expressed by $\Delta\beta_c t$, $1 - \Delta(t)$ may be approximated by $e^{-(\Delta\beta_c)t}$ to give $C_2(t) \simeq e^{-(\beta_c+\Delta\beta_c)t}$ up to $t = 5/\gamma_A$, keeping the exponential decay behaviour. But for much larger t, $C_2(t)$ will show different behaviour.

Finally we briefly discuss the possible applications of our findings in this paper. In the study of laser–plasma interaction, the spontaneous emission rates of ions are widely used for the absolute intensity measurements of spectral lines in the vacuum ultraviolet wavelength region (the branching-ratio technique) [14, 15]. We have shown that the relativistic correction and finite atom-size correction to the spontaneous emission rate can be quite large for ions of large Z. Inclusion of such corrections can improve the accuracy of the absolute intensity measurements. More recently, trapped ions have been proven to constitute a model system for storing and processing quantum information. The transport of this information within distributed quantum networks requires an interface between trapped ions and photons operating as moving quantum bits. Such an interface could be based on the deterministic coupling of a single ion to a high finesse optical cavity, which requires a precise control of the spontaneous emission properties of the ion [16, 17]. Our result on the spontaneous emission rate of ions may be helpful to the study of spontaneous emission of single trapped ions.

Acknowledgment

This work is supported by the National Science Foundation of USA(DMR-0093949).

References

[1] Weisskopf V and Wigner E 1930 *Z. Phys.* A **63** 54
[2] Paley R and Wiener N 1934 *Fourier Transforms in the Complex Domain* (*Am. Math. Soc. Colloq. Publ. 19*) (Providence, RI: American Mathematical Society)
[3] Knight P L and Milonni P W 1976 *Phys. Lett.* A **56** 275
[4] Wodkiewicz K and Eberly J H 1976 *Ann. Phys.* **101** 574
[5] Carrazana P and Vetri G 1980 *Nouvo Cimento* B **55** 191
[6] Robisco R T 1984 *Phys. Lett.* A **100** 407
[7] Seke J and Herfort W 1988 *Phys. Rev.* A **38** 833
Seke J and Herfort W 1989 *Phys. Rev.* **40** 1926
[8] Seke J 1992 *J. Phys. A: Math. Gen.* **25** 691
Seke J 1997 *Physica* A **238** 338
Seke J 1998 *Phys. Lett.* A **244** 111
[9] Cao C-Q, Long W, Wei J and Cao H 2001 *Phys. Rev.* A **64** 043810
[10] Cao C-Q, Tian J-R and Cao H 2002 *Phys. Lett.* A **303** 318
[11] See, for example Carmichael H J 1993 *An Open System Approach to Quantum Optics* (*Springer Lecture Notes in Physics M* vol 7) (Berlin: Springer)
[12] Imamoglu A 1994 *Phys. Rev.* A **50** 3650
[13] Cao C-Q, Yu C-G and Cao H 2003 *Eur. Phys. J.* D **23** 279
[14] Hinnov E and Hofman F 1963 *J. Opt. Soc. Am.* **53** 1259
[15] Chung Y, Lemaire P and Suckewer S 1988 *Phys. Rev. Lett.* **60** 1122
[16] Guthohrlein G R *et al* 2001 *Nature* **414** 49
[17] Kreuter A *et al* 2004 *Phys. Rev. Lett.* **92** 203002